Brief communication: Updated grounding line mapping in the Amundsen Sea Embayment, Antarctica, from 1-day repeat Sentinel-1 SAR data

Jonas K. Andersen[1], Romain Millan[2], Eric Rignot[3,4], Lucille Gimenes[2], Bernd Scheuchl[3], Jean Baptiste Barré[3], and Anders A. Bjørk[1]

[1]Department of Geosciences and Natural Resource Management, University of Copenhagen, 1350 Copenhagen, Denmark
[2]Univ. Grenoble Alpes, CNRS, IRD, INRAE, Grenoble-INP, IGE (UMR 5001), 38000 Grenoble, France
[3]Department of Earth System Science, University of California, Irvine, CA 92697
[4]Radar Science and Engineering Section, Jet Propulsion Laboratory, California Institute of Technology, Pasadena, CA 91109

Correspondence: Jonas K. Andersen (joka@ign.ku.dk)

Abstract. Knowledge of Antarctic glacier grounding lines, which mark the transition between grounded and floating ice, is a vital parameter in determining the stability of major ice shelves and hence the ice sheet. Rapid grounding line retreat and associated mass loss has been documented at numerous Antarctic glaciers, particularly in the Amundsen Sea Embayment. However, few comprehensive grounding line mappings exist, particularly from recent years. Here, we utilize a unique record of Sentinel-1 Synthetic Aperture Radar 1-day repeat-pass imagery to generate a comprehensive retrieval of grounding line location in the Amundsen Sea Embayment in 2025 and evaluate recent changes.

1 Introduction

Mass loss from the Antarctic Ice Sheet has increased over the past four decades, mainly due to speed-up and increased ice discharge of glaciers in West Antarctica (Otosaka et al., 2023). Mass loss from this sector increased from 39.5 ± 19 Gt/y during 1992-2001 to 103.6 ± 10.8 Gt/y during 2002-2020 (Otosaka et al., 2023). Glacier acceleration is linked to ice shelf weakening, driven by the intrusion of warm, saline circumpolar deep water beneath floating ice, which enhances basal melting (Holland et al., 2023). Melting peaks near the grounding line (GL), the boundary between grounded and floating ice. As ~~ocean temperatures rise~~warm and saline circumpolar deep water is advected below the ice shelf, GL retreat into deeper basins accelerates ice flow and dynamic thinning, further promoting retreat and decreasing the buttressing potential of ~~ice shelves~~ the shelf (Schmidtko et al., 2014; Holland et al., 2023; Joughin et al., 2014). In the Amundsen Sea Embayment (ASE), located at the West Antarctic Ice Sheet (Figure 1) and holding a ~~1.2~~ 1.26 ± 0.02 m potential sea level rise (Morlighem et al., 2020), monitoring of ~~grounding lines~~ GL locations is of particular interest due to their documented rapid retreat into drainage basins deep below sea level, which will likely lead to further instabilities and mass loss in the future (Mouginot et al., 2014; Park et al., 2013; Rignot et al., 2014; Scheuchl et al., 2016).

Given the ~~grounding line~~GL's critical role in Antarctic ice sheet stability and mass loss, accurate information on its evolution is essential for better constraining ice-ocean interactions and predicting the ice sheet's future evolution and its contribution to

sea-level rise. Thus, extensive and repeated observations of this critical boundary are essential (Konrad et al., 2018; Rignot, 2023). The need for frequent observations is compounded by the fact that the true GL fluctuates during a tidal cycle within ~~a~~ an ice grounding zone, which may be several kilometers wide, depending on factors such as tide magnitude, ice thickness, and bedrock slope ~~(Fricker and Padman, 2006)~~(Fricker and Padman, 2006; Freer et al., 2023; Milillo et al., 2022; Rignot et al., 2024).

While in-situ methods for observing ~~grounding line~~ GL location have been demonstrated (e.g., Le Meur et al. (2014)), remote sensing techniques offer a more feasible alternative for large-scale, repeated retrievals. Several remote sensing techniques have been applied including phase-based and amplitude-based processing of satellite Synthetic Aperture Radar (SAR) data, repeat laser or radar altimetry, and optical imagery - a comprehensive review of these methods ~~are~~ is provided by Friedl et al. (2020). The most accurate retrievals are obtained from double-difference SAR interferometry (Rignot, 1996; Friedl et al., 2020) (described in section 2.2). This technique has been used to map ~~grounding lines~~ GLs across the Antarctic Ice Sheet, with the ERS-1/2 satellites allowing for a particularly extensive coverage, however only during periods where the satellites flew in short repeat-pass constellations (i.e., the 1-day tandem phases during 1995-1996 and 1999-2000 and the 3-day ice phases during 1991-1992, 1994, and 2011) (Rignot et al., 2016). While the temporal resolution of these acquisitions was limited to discrete intervals, precluding a full delineation of the grounding zone, the ERS imagery enabled the detection of rapid and widespread ~~grounding line~~ GL retreat across West Antarctica during the 1991–2011 period (Rignot et al., 2014). Recent advances using data from the Sentinel-1 archive provided ~~an~~ a continent-wide estimate of the grounding zone, through a dense time series of automated interferometry-based GL retrievals from 2018 (Mohajerani et al., 2021). However, this retrieval was limited by the relatively long repeat-pass period of Sentinel-1 (6 or 12 days), hindering delineations in the fastest-changing sectors, where strong decorrelation occurs in central glacier trunks experiencing the highest GL retreat. Some previous studies have acquired commercial/non-public SAR data with short repeat-pass periods to provide well-resolved GL retrievals over specific glaciers (e.g., Rignot et al. (2024); Milillo et al. (2022)). However, no public, routinely acquired SAR data with a repeat-pass period short enough to provide adequate GL delineations over the fastest-changing glaciers in the ASE currently exists.

Here, we use Sentinel-1 imagery with a 1-day repeat-pass period, acquired during January-March 2025 for the in-orbit commissioning of Sentinel-1C, to delineate glacier ~~grounding lines across the Amundsen Sea Embayment~~GLs across the ASE. The short repeat-pass data allows for ~~a~~ several well-resolved, contemporary ~~delineation of ASE grounding lines~~delineations of ASE GLs, most of which have been mapped only rarely in the past decade and, to our knowledge, not at all since 2020 or earlier.

2 Data and methods

2.1 Sentinel-1 data

The EU Copernicus Sentinel-1 satellite constellation nominally consists of two C-band SAR satellites, orbiting in a polar, sun-synchronous orbit 180 degrees out of phase. The orbit repeat-pass period is 12 days, yielding a 6-day repeat-pass period with two active satellites. Sentinel-1A, launched in April 2014, remains active, while Sentinel-1B (launched in July 2016) ceased

operations on 23 December 2021 due to a power system failure. Consequently, dense 6-day repeat-pass coverage was available across the Antarctic and Greenland ice sheet margins from 2016 to 2021. From 2022 to early 2025, the constellation operated with only Sentinel-1A, yielding 12-day temporal baselines. The launch of Sentinel-1C on 5 December 2024, followed by its in-orbit commissioning (completed in May 2025), restored 6-day repeat coverage. Sentinel-1D ~~is currently planned for launch in late~~ was successfully launched on 4 November 2025~~to replace 1A, which has exceeded its expected lifetime~~, and is currently undergoing in-orbit commissioning.

A short temporal baseline (i.e., the time separation of images) in interferometric SAR processing is vital, as increased baselines generally lead to increased decorrelation. In many parts of the marginal Antarctic and Greenland ice sheets ~~,~~ high flow speeds, shear deformation, snowfall and redistribution, and/or surface melt yield total decorrelation for 6- or 12-day Sentinel-1 image pairs all year, ~~excluding~~ precluding the retrieval of flow speeds or ~~grounding line~~ GL delineations.

During the in-orbit commissioning phase of Sentinel-1C, the satellite was temporarily placed in a 1-day offset orbit relative to Sentinel-1A from January 17th to March 7th 2025. A total of 166 Single Look Complex image slices, covering four orbit tracks (see Figure S1) in the Interferometric Wide swath mode, were acquired from both satellites over the marginal Antarctic Ice Sheet in the ~~Amundsen Sea Embayment (Figure~~ ASE (Figures 1). These 1-day repeat retrievals form the basis of our updated 2025 ~~grounding line delineation~~GL delineations.

2.2 Double-difference interferometry for grounding line detection

Differential SAR interferometry (DInSAR) measures the phase difference between two subsequent SAR acquisitions, which, after correcting for satellite geometry and surface topography (using a Digital Elevation Model), is proportional to surface displacement in the radar line-of-sight (LoS) direction (Massonnet et al., 1993). Because the LoS vector has both vertical and horizontal components, phase changes can reflect motion in either direction:

$$\Delta\phi^1_{LoS} = \Delta\phi^1_{horz} + \Delta\phi^1_{vert} \tag{1}$$

By differencing two sequential DInSAR measurements, a technique known as double-difference interferometry, we isolate changes in LoS displacement between the two time intervals. If horizontal velocity remains steady, these differences primarily reflect changes in vertical displacement:

$$\Delta\phi^{DD}_{LoS} = \left(\Delta\phi^2_{horz} + \Delta\phi^2_{vert}\right) - \left(\Delta\phi^1_{horz} + \Delta\phi^1_{vert}\right) = \Delta\phi^2_{vert} - \Delta\phi^1_{vert} \tag{2}$$

Over floating ice shelves, tidal variations between acquisitions often produce different vertical motion contributions between repeat passes, leading to measurable double-difference phase signals in the form of dense fringes, while the (presumed) constant horizontal flow contribution cancels out. The inland limit of these fringes marks the limit of tidal flexure of the ice, which approximately coincides with the ~~grounding line~~GL, although the true ~~grounding line~~ GL will generally lie slightly seaward of the flexure limit (Fricker and Padman, 2006). This approach is widely regarded as one of the most accurate remote sensing

methods for ~~grounding line~~ GL detection and has been applied with various SAR sensors (Rignot, 1996; Joughin et al., 2010; Friedl et al., 2020).

Differential interferograms were processed using the workflow outlined in Andersen et al. (2020). The REMA DEM at 100 m resolution (Howat et al., 2022) and MEaSUREs Antartica Ice Velocity product at 450 m resolution (Rignot et al., 2017) were applied in the refined coregistration procedure, and all images from each respective track were resampled to the same reference image. We use Precise Orbit Ephemerides (POE) to update orbit state vectors only for Sentinel-1A acquisitions, as POE products for Sentinel-1C were not available for this period. Finally, double-difference interferograms are then formed simply by differencing the phase images of sequential interferograms.

~~Grounding lines~~ GLs were manually digitized at the inland limit of the tide-induced fringe patterns (see Figure 2). ~~For some areas, multiple~~ A separate delineation was generated for each available double-difference ~~interferograms are available due to multiple acquisition cycles from the same track or overlapping of different orbit tracks. In those cases, we generally select the most coherentretrieval, that best resolves grounding line features , for delineating the grounding line~~interferogram, digitizing all resolvable (coherent) GL features within the given product. We also digitize pinning points, i.e. localized areas of the ice shelf that stick to bathymetric highs and act to buttress and stabilize ice flow.

3 Results

Figure 1 shows an overview of the 2025 ~~Amundsen Sea Embayment grounding line from the~~ ASE GL delineations from available Sentinel-1 1-day repeat imagery ~~. The delineation spans from the~~ (see Table S1), spanning the coast from Abbot Ice Shelf to ~~the~~ Getz Ice Shelf. Figure 2 shows examples of Sentinel-1 1-day double-difference interferograms ~~for the four~~ and associated GL delineations for four of the regions highlighted in Figure 1. The interferograms are generally highly coherent and ~~a contiguous grounding line is delineated~~ at least one contiguous GL delineation was mapped for nearly the entire coast, with a few exceptions in zones of high velocity gradients at Thwaites, Pine Island, and Kohler glaciers, which lead to decorrelation even with the 1-day repeat pass period. For the majority of the region, multiple GL delineations were made spanning different tidal and atmospheric conditions (Text S1, Table S1). GLs near the Abbott and Cosgrove ice shelves were captured in 1-2 delineations, while the remaining regions were captured in 3-7 separate retrievals. While this sampling density is insufficient to robustly resolve the full grounding zone, the availability of multiple delineations enables partial observation of short-term, tide- and pressure-induced GL variability. Examples of such short-term GL migration, varying from a few hundred meters to several kilometers, are shown in Figure S2.

Figure 3 shows a comparison between the new 2025 ~~grounding line delineation~~ GL delineations and the MEaSUREs Antarctica grounding line product (Rignot et al., 2016), which contains retrievals from the period 1992-2014 for nearly the full region, the ESA CCI grounding line product (ESA AIS CCI, 2021), containing retrievals from the period 1994-2020 for select glaciers, and the COSMO-SkyMed grounding line dataset from Milillo et al. (2022), covering the Pope, Smith, and Kohler ~~Glaciers~~ glaciers during 2016-2020, ~~depending on which product contains the latest well-resolved delineation for the given glaciers. The grounding lines are~~ overlaid on the BedMachine v3 bed elevation product (Morlighem, 2022). ~~In the ASE sector, estimates~~

These historic GL products generally rely on single or sporadic acquisitions per year and therefore represent snapshots of the GL at varying tidal and atmospheric conditions, rather than the full grounding zone. In contrast, the deep learning-based 2018 GL dataset of Mohajerani et al. (2021), although not covering the fastest-flowing glaciers (e.g., Pine Island, Thwaites, Smith), provides an estimate of grounding zone width ~~are mostly around~~ based on all available 2018 Sentinel-1 data. In the ASE, grounding zone widths inferred from this product vary from less than 1 km ~~but may locally exceed~~ to locally more than 5 km~~(Mohajerani et al., 2021). Consequently, the reported changes in GL location should be viewed as approximative, as they stem from a comparison of discrete acquisitions.~~ .

Taken together, these differences in temporal sampling imply that apparent GL advances or retreats between products, particularly between single-acquisition historic delineations and the 2025 retrievals, should be interpreted with caution. Where offsets of several kilometers are observed, part of the apparent change may reflect the incomplete capturing of the grounding zone, rather than solely long-term migration. The 2025 dataset occupies an intermediate position between single-acquisition historical products and fully resolved grounding zone estimates, providing improved, although partial, constraints on short-term GL variability.

At Abbot Ice Shelf, which extends from the Bellingshausen Sea into the ASE, the GL remains almost completely unchanged since the 1990s, with the 2025 delineation lying within $\pm$1 km of the 1992/1995 position almost everywhere (Figure 3a), which in turn aligns well with the 2018 grounding zone (Mohajerani et al., 2021). Christie et al. (2016) found a widespread but modest ~~grounding line~~ GL retreat during 1990-2015 ($<$1 km for most sectors but locally as high as 3 km). Such a retreat does not appear to have continued into the 2015-2025 period. The locations of pinning points observed in 2025 remain nearly identical to the 1992/1995 positions (Figure 3a). Owing to its stability relative to the neighboring ice shelves in the ASE, the Abbot Ice Shelf remains less studied, however, previous work has identified an onset of dynamic thinning following a flow speed-up at the grounding zone (Chuter et al., 2017), and the ice shelf has been suggested to be vulnerable to incoming warm circumpolar deep water (Christie et al., 2016). The 2025 GL delineations also provide coverage over nearly the entire coast of Thurston Island (Figure 1), most of which is not captured in historic products (Rignot et al., 2016; ESA AIS CCI, 2021).

Similarly, the neighboring Cosgrove Ice Shelf shows no apparent GL changes since the ~~1992-2011~~ 1992-2018 period, with the 2025 delineation lying within a few hundred meters of the 2011 retrieval almost everywhere (Figure S3a-b). An exception is observed in the central, fastest-flowing trunk, where the 2025 GL lies 1-2 km inland from the 2011 delineation~~(Figure S2a-b)~~, although still remaining well within the 2018 grounding zone, which is observed to be wider in this sector (Mohajerani et al., 2021). The apparent stability is not surprising, as the Cosgrove ~~grounding line~~ GL is situated on a predominantly prograde bed (Figure ~~S2b).~~ S3b). Only a single double-difference interferogram could be generated for this region, so any short-term, tide-induced GL migration is not captured by our product.

The fastest-flowing sector of the Getz Ice Shelf is not covered by the Sentinel-1 1-day repeat data set. For the rest of the ice shelf, we compare the 2025 GL ~~delineation~~ delineations with the 2018 retrievals from Mohajerani et al. (2021) and note that the 2025 GL lies approximately within the estimated 2018 grounding zone, with a few local exceptions, in which the 2025 GL ~~lies~~ appears to lie 1-2 km inland (Figure ~~S2c-d~~S3c-d).

At Pine Island Ice Shelf, the main trunk ~~grounding line has shown a~~ GL shows an apparent further retreat of approximately 2-7 km since 2011, following a larger retreat of 15-20 km during 1992-2011. In the main trunk of the glacier - the region with the fastest ice flow - the ~~western~~ northern section has retreated by up to 7 km, while the central part has pulled back by approximately ~~2.5~~ 1-3 km. The ~~western~~ southern section of the main trunk appears to have been dislodged from a sill in the bedrock topography at a depth of -1000 m and ~~has~~ subsequently retreated by around 5 km (Figure 3b). In this critical part of the glacier, where ice discharge is at its maximum, the GL has retreated more significantly along the ~~eastern and western~~ northern and southern flanks than at the center. The ~~eastern branch of Pine Island~~ southern tributary glacier, sometimes referred to as Piglet Glacier, which flows toward the ~~ice shelf~~ Pine Island Ice Shelf front, has ~~also experienced a grounding line retreat averaging around 5 km ,~~ experienced widespread GL retreat during 2016-2018, averaging around 3 km with localized retreats reaching up to ~~7~~ 6 km, particularly in areas where the bedrock slope is slightly retrograde. ~~On the western flank of the ice shelf, however, the grounding line~~ In 2025, we observe an additional apparent retreat of around 2 km, compared to the 2018 grounding zone (Figure 3b). Conversely, at the northern tributaries (Lucchitta and Larter glaciers), the GL has remained relatively stable, situated on a more pronounced, mountainous, and prograde topography (Figure 3b). Finally, the 2025 interferograms show the presence of a pinning point in the central part of the ice shelf (Figure 2b), which has previously been identified as an ephemeral feature (Qian et al., 2025; Rignot et al., 2014).

The Thwaites Ice Shelf ~~grounding line~~ GL has shown a spatially varying retreat since 1992, ranging from <1 km to 20 km, (Milillo et al., 2019; Rignot et al., 2014, 2024). The highest retreat rates are associated with ice shelf basal channels, which enhance basal melt rates, and steep retrograde bed slopes (Chartrand et al., 2024). ~~The 2025 grounding line delineation~~ In the eastern sector, where the ice shelf is largest, we observe local retreats spanning 3-8 km, when comparing to the 2018 grounding zone (Mohajerani et al., 2021). In the western sector, the 2025 GL delineations (Figure 3c) ~~lies~~ lie within the 2023 grounding zone measured by ~~(Rignot et al., 2024)~~ Rignot et al. (2024) using commercial ICEYE data. Loss of coherence in parts of the fastest-flowing sector leads to local discontinuities in the 2025 ~~delineation~~delineations. We observe indications of apparent seawater intrusions behind the Thwaites GL, which may enhance basal melting under grounded ice, in the same ~~locations~~ location reported by Rignot et al. (2024) in March-June 2023 (~~Figure S3~~Figures 2c and S4), suggesting that these intrusions persistently reoccur. Recent work ~~has~~ also documented how subglacial discharge from upstream lake drainages ~~temporarily enhances~~ previously enhanced ocean melting near the ~~grounding line~~GL in the same sector as the observed seawater intrusions, promoting further retreat (Gourmelen et al., 2025).

Figure 3d shows an overview of the system of Pope, Smith, and Kohler glaciers, which feed the Crosson and Dotson ~~Ice Shelves~~ice shelves. At the main trunk of Pope Glacier, the 2025 ~~grounding line~~ GL remains at the 2018-2020 position, following an apparent 6 km retreat during 2014-2018 (and a ∼15 km retreat during 1996-2014). Scheuchl et al. (2016) noted that a prograde bedrock slope beginning 4.5 km behind the 2014 GL position might limit further ~~grounding line~~ GL retreat, perfectly in line with our observations. A similar pattern is observed at Smith Glacier. Both of the Smith East and Smith West ~~grounding lines~~ GLs remain at their 2018-2020 positions, following a 5-6 km retreat during 2014-2020. Both ~~grounding lines~~ GLs now sit at flat or slightly prograde bed slopes, after having retreated past retrograde slopes during 1992-2016 (Scheuchl

et al., 2016; Milillo et al., 2022). Contrary to Pope, however, both Smith East and Smith West will encounter retrograde bed slopes again if GL retreat continues another 3-7 km (Figure 3d).

The Kohler Glacier ~~grounding line~~ GL retreated 8 km during 1992-2011, re-advanced 4.5 km during 2011-2014, then retreated 7 km during 2014-2020. The 2025 ~~grounding line~~ GL now sits approximately at the 2018-2020 position, about 3 km from the top of a steep prograde slope (Milillo et al., 2022).

The abated ~~grounding line~~ GL retreat during 2018-2025 of Pope, Smith, and Kohler (compared to the preceding decades) is associated with a shift in the ice flow regime: Selley et al. (2025) observed near-steady flow speeds during the 2015-2022 period for all glaciers, whereas all glaciers showed rapid flow acceleration for all or parts of the 2005-2015 period.

~~Additionally, The Dotson ice shelf also appears to have lost two pinning points since 2016. Furthermore, many smaller glaciersin the region, including Philbin Inlet, Singer Glacier, and McClinton glaciers , also show grounding line retreats in the range of 2-6 kmsince their latest delineation from the MEaSUREs dataset, although their~~ Finally, we note apparent GL retreat at a series of smaller glaciers, including Bunner, Holt, McClinton, Singer, and Philbin Inlet glaciers (Figure S5). These glaciers generally exhibit wide grounding zones (5-10 km), as estimated from 2018 data (Mohajerani et al., 2021), complicating the prescription of long-term migration based on few observations. However, we note that all 2025 GL ~~positions do appear to lie within (or near) the estimated~~ delineations (3-5 retrievals per glacier) lie at the inland limit of the 2018 grounding zones~~from Mohajerani et al. (2021).~~ , with only a small fraction (or none) of the 2018 delineations extending comparably far inland, suggesting a potential modest retreat. The clearest example is Holt Glacier, for which 2025 delineations lie 2-3 km inland of any 2018 retrievals (Figure S5a).

4 Conclusions

Continually updated retrievals of glacier ~~grounding lines~~ GLs are essential for understanding the ongoing rapid mass loss from the ASE as well as detecting early signs of retreat and instability at other ice shelves (Li et al., 2023; Brancato et al., 2020; Milillo et al., 2019; Millan et al., 2022). Existing spatially comprehensive GL products are based primarily on data from ERS-1/2, Sentinel-1, and TerraSAR-X/TanDEM-X with additional retrievals from Radarsat-1/2, ALOS PALSAR, and COSMO-SkyMed (Rignot et al., 2016; Mohajerani et al., 2021; Milillo et al., 2022; ESA AIS CCI, 2021). The vast majority of well-resolved, contiguous ~~grounding line~~ GL delineations, however, come from short repeat-pass SAR acquisitions, such as ERS-1/2 imagery from the tandem mission phase (1-day repeat-pass, 1995-1996 and 1999-2000) and the ice phase (3-day repeat-pass, winters of 1991/1992 and 1993/1994 and 2011) (Rignot et al., 2016; Friedl et al., 2020). Other studies have used short repeat-pass data from non-public/commercial SAR satellites, allowing for highly resolved GL retrievals at specific glaciers (e.g., Milillo et al. (2019); Rignot et al. (2024)). No current satellite mission provides publicly available, short (<6 days) repeat-pass SAR data, and no sensors acquire routine short repeat-pass data with a large-scale (i.e., ice sheet-wide) coverage. This lack of short-repeat pass data remains the limiting factor for routinely retrieving ~~grounding line locations, specifically~~ GL locations, particularly for the most vulnerable and rapidly changing regions of the ice sheet (Friedl et al., 2020). In this context, the Sentinel-1 1-day repeat-pass acquisition campaign during the Sentinel-1C commissioning phase

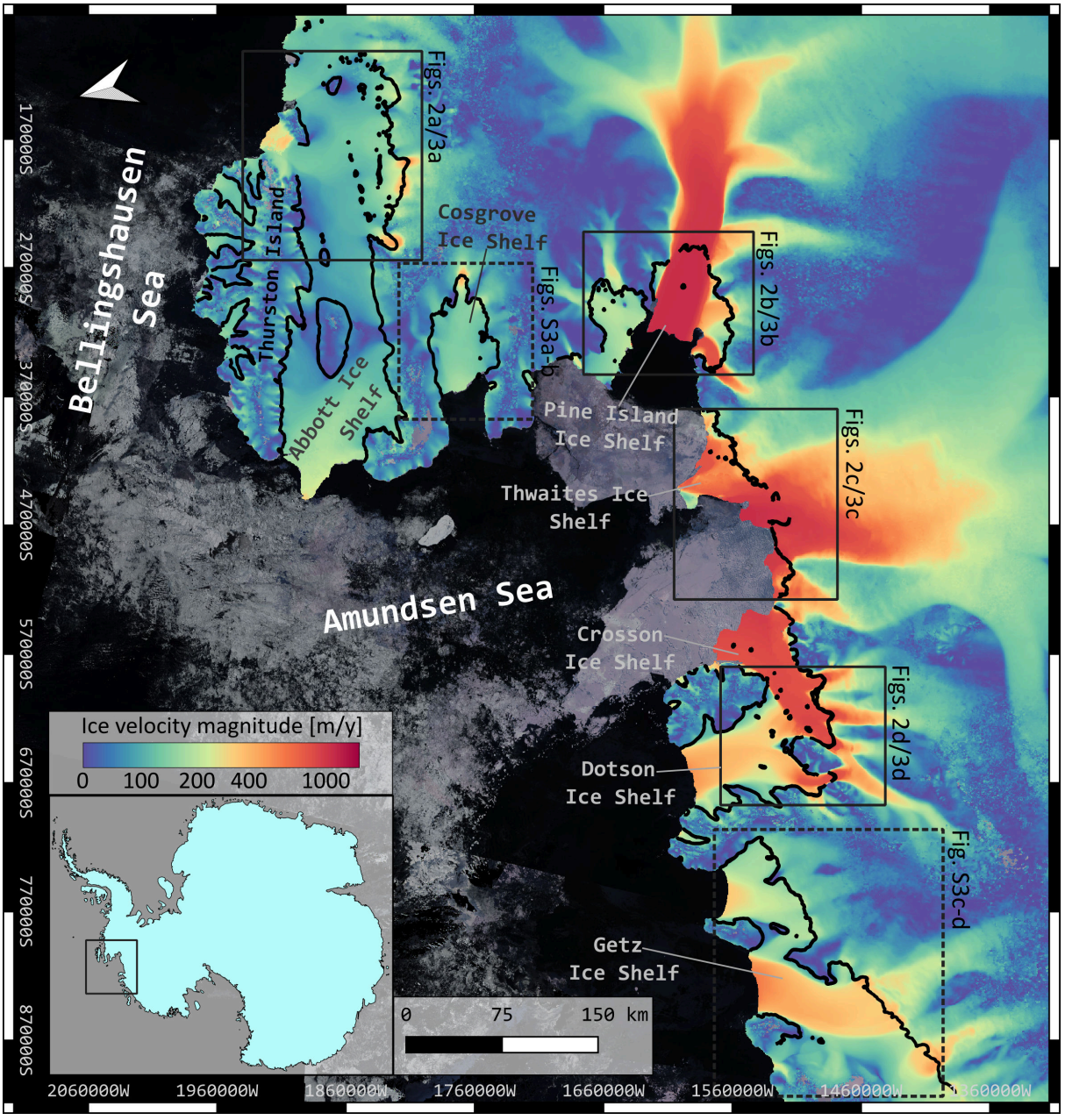

Figure 1. Overview of Sentinel-1 2025 Amundsen Sea Embayment grounding line ~~delineation~~ delineations (black ~~line~~lines), overlaid on an ice velocity mosaic from MEaSUREs (Rignot et al., 2017), clipped to the 2025 ice shelf extent (as derived from Sentinel-1 intensity images). Black rectangles indicate spatial extents of panels (a)-(d) in Figures 2 and ~~3.~~3, while dashed rectangles show extents for Figure S3. Background map is a Sentinel-2 true color mosaic from January-March 2025 and map projection is EPSG:3031 (arrow in top left corner shows true north.)

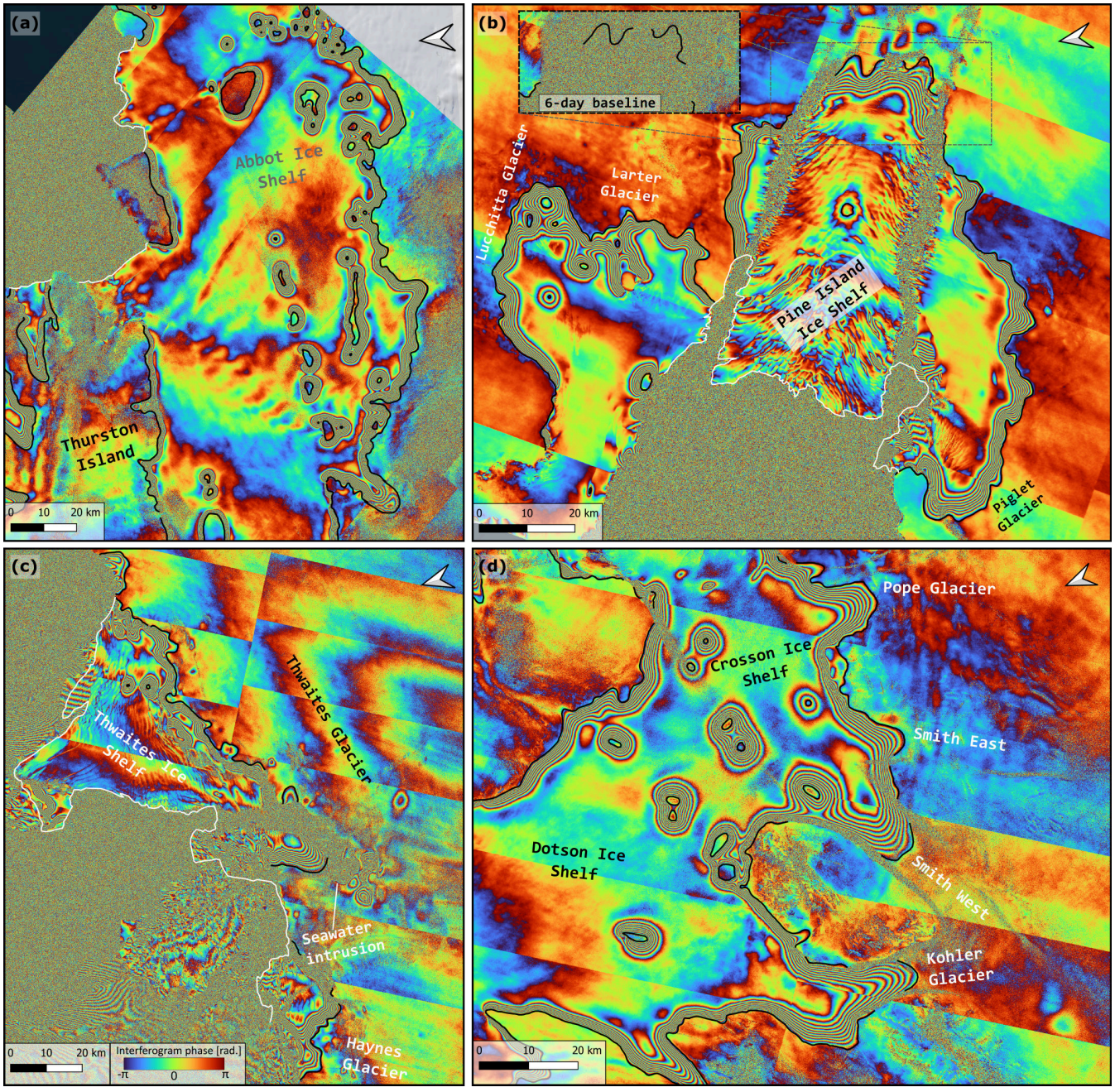

Figure 2. Sentinel-1 1-day repeat double-difference interferograms from 2025 covering Abbot Ice Shelf (a), Pine Island Ice Shelf (b), Thwaites and Haynes glaciers (c), Pope, Smith, and Kohler glaciers (d). Acquisition ~~dates~~ times and ~~orbit track numbers~~ corresponding relative and maximum sea surface height estimates (Text S1) are provided in Table S1~~in the Supplementary Material~~. ~~The 2025~~ Sentinel-1 2025 grounding line ~~product is~~ delineations are indicated by black lines. ~~The dense fringe patterns arise from differences~~ Inset in ~~the tide-induced vertical flexure between grounded and floating ice. The inland limit of this flexure is interpreted as the~~ (approximateb) ~~grounding line. The interferograms also reveal pinning points~~ contains an example double-difference interferogram using 6-day baseline imagery (~~in the form of local, circular fringe patterns~~Figure S6), which shows complete loss of coherence. White lines show 2025 ice shelf calving fronts and top right arrows indicate true north.

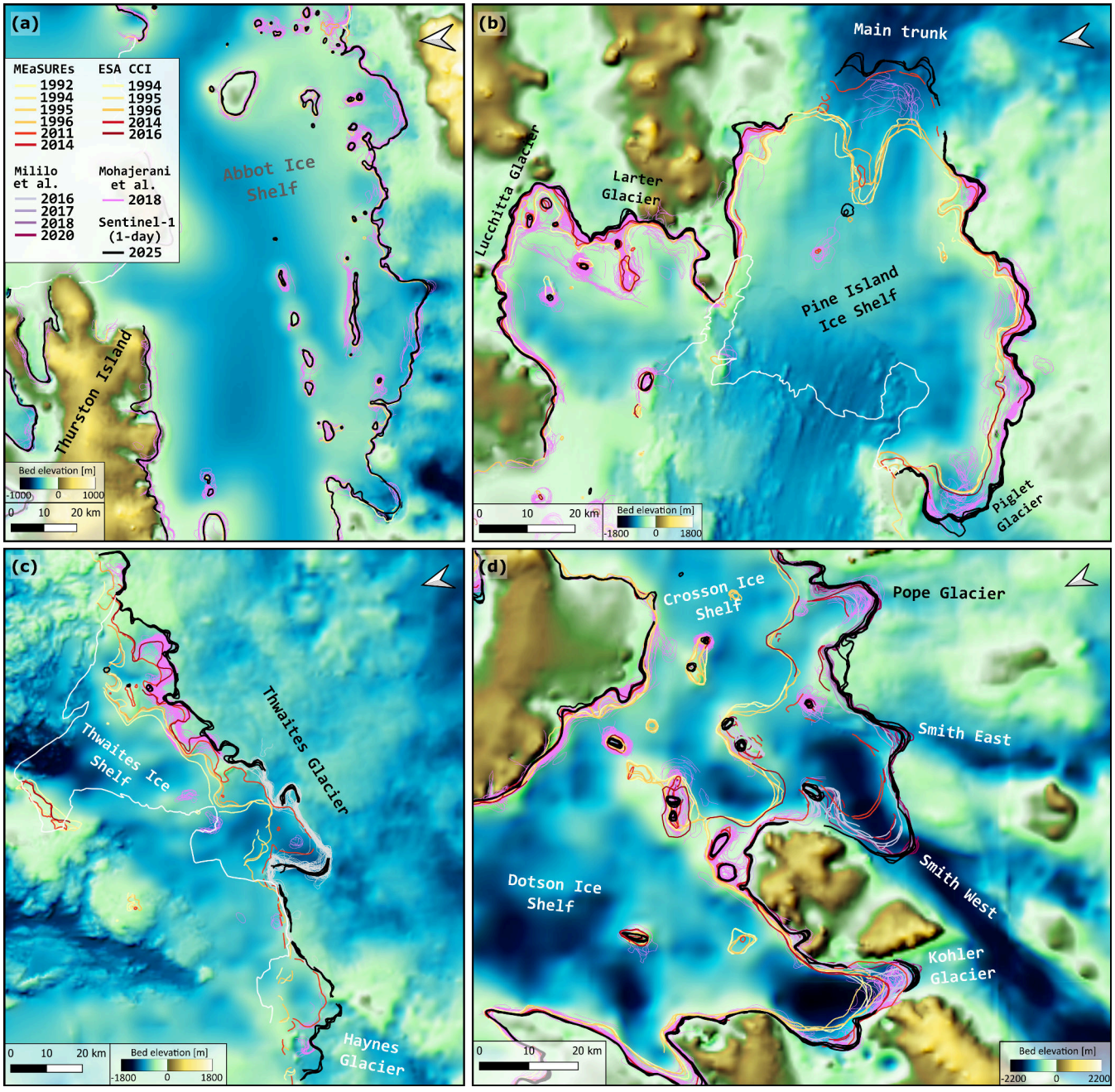

Figure 3. Grounding line changes at Abbot Ice Shelf (a), Pine Island Ice Shelf (b), Thwaites and Haynes glaciers (c), Pope, Smith, and Kohler glaciers (d). Background map shows bed elevation from BedMachine v3 (Morlighem, 2022) and white lines indicate 2025 ice shelf calving fronts. The 2025 Sentinel-1 grounding line product is indicated by ~~orange~~ black lines, while the MEaSUREs (Rignot et al., 2016), ~~ESA CCI (ESA AIS CCI, 2021)~~ESA AIS CCI (2021), ~~and~~ Mililo et al. (2022), and Mohajerani et al. (2021) grounding line products are indicated by various colors, depending on ~~the~~ retrieval year (see legend in panel (a)). Grey lines in (c) show grounding line delineations from Rignot et al. (2024).

clearly demonstrates the potential for operational short-repeat SAR acquisitions in large-scale, high-resolution ~~grounding line~~ ~~monitoring. Figure S4 illustrates~~ GL monitoring. Figures 2c and S6 illustrate the significant improvement in coherence achieved with 1-day repeat data compared to longer baseline interferograms. The launch of Sentinel-1D may provide another opportunity for acquiring 1-day repeat imagery and hence ~~grounding line~~ GL delineations similar to the ~~one~~ ones presented here.

We have presented a 2025 grounding line ~~delineation~~ dataset in the Amundsen Sea Embayment featuring multiple acquisitions with near-contiguous coverage, based on a, to date, unique set of Sentinel-1 1-day repeat-pass data. ~~Grounding lines~~ GLs in the ASE have been mapped with a relatively coarse temporal resolution over the past three decades and, to our knowledge, the vast majority of ~~grounding lines~~ GLs have not been mapped since the 2018-2020 period ~~(Mohajerani et al., 2021)~~ (Mohajerani et al., 2021; Milillo et al., 2022), so the 2025 ~~delineation~~ dataset serves as an important acquisition in maintaining a consistent time series for the region. Future GL retrievals will be needed to monitor both the ongoing retreat at glaciers such as Pine Island and Thwaites as well as the potential onset of ~~grounding line~~ GL retreat, and hence instability, at other ice shelves such as Abbot, Cosgrove, and Getz.

The 2025 ~~grounding line retrieval highlights~~ GL retrievals highlight areas of continued vulnerability, particularly at Pine Island and Smith ~~Glaciers~~glaciers, where the ~~grounding lines~~ GLs are situated at or near retrograde bed slopes. At Pine Island, retreat into deeper terrain will further enhance discharge, while continued retreat at Smith could soon lead to renewed instability as the glacier enters another retrograde section of the bed. These configurations emphasize the value of high-resolution, repeated ~~grounding line mapping~~ GL observations to track evolving glacier stability.

Data availability. The 2025 Amundsen Sea Embayment grounding line product, along with geocoded Sentinel-1 double-difference interferograms used for delineations, is available at https://doi.org/10.5281/zenodo.18503724. Sentinel-1/2 imagery, including Precise Orbit Ephimeredes, is available at https://dataspace.copernicus.eu/. The MEaSUREs Antarctica grounding line product is available at https://doi.org/10.5067/IKBWW4RYHF1Q (Rignot et al., 2016) and the ESA CCI Antarctica grounding line product is available at https://climate.esa.int/en/projects/ice-sheets-antarctic/ (ESA AIS CCI, 2021). The MEaSUREs Antarctica velocity mosaic is available at https://doi.org/10.5067/D7GK8F5J8M8R (Rignot et al., 2017), the BedMachine v3 bed elevation product is available at https://nsidc.org/data/nsidc-0756/versions/3 (Morlighem, 2022), and the REMA Digital Elevation Model is available at https://doi.org/10.7910/DVN/EBW8UC (Howat et al., 2022).

Author contributions. J.K.A., A.A.B., and E.R. designed the study. J.K.A., J.B.B., and L.G. carried out data processing, with analysis contributions from all authors. J.K.A wrote the initial draft of the manuscript, with editing from all other authors.

Competing interests. The authors declare no competing interests.

Acknowledgements. We thank Nuno Miranda and ESA for publicly providing the 1-day repeat Sentinel-1 data. J.K.A. and A.A.B. acknowledge support from the Villum Foundation (Villum Young Investigator grant no. 29456) and the Independent Research Fund Denmark Sapere Aude Research Leader grant (10.46540/2064-00050B). R.M acknowledges support from the European Research Council (ERC) under the Horizon Framework research and innovation program of the European Union (grant no. 101164392; "IceDaM" project). The work was partially performed at the University of California Irvine and Caltech Jet Propulsion Laboratory under a contract with the National Aeronautics and Space Administration Cryosphere Science (80NSSC23K0177), MEaSUREs (80NSSC23M0146), and MAP (80NSSC20K1076) programs and the National Science Foundation Thwaites-MELT (1739003).

References

Andersen, J. K., Kusk, A., Boncori, J. P. M., Hvidberg, C. S., and Grinsted, A.: Improved Ice Velocity Measurements with Sentinel-1 TOPS Interferometry, Remote Sensing, 12, 2014, https://doi.org/10.3390/rs12122014, 2020.

Brancato, V., Rignot, E., Milillo, P., Morlighem, M., Mouginot, J., An, L., Scheuchl, B., Jeong, S., Rizzoli, P., Bueso Bello, J. L., and Prats-Iraola, P.: Grounding Line Retreat of Denman Glacier, East Antarctica, Measured With COSMO-SkyMed Radar Interferometry Data, Geophysical Research Letters, 47, e2019GL086 291, https://doi.org/10.1029/2019GL086291, 2020.

Chartrand, A. M., Howat, I. M., Joughin, I. R., and Smith, B. E.: Thwaites Glacier thins and retreats fastest where ice-shelf channels intersect its grounding zone, The Cryosphere, 18, 4971–4992, https://doi.org/10.5194/tc-18-4971-2024, 2024.

Christie, F. D. W., Bingham, R. G., Gourmelen, N., Tett, S. F. B., and Muto, A.: Four-decade record of pervasive grounding line retreat along the Bellingshausen margin of West Antarctica, Geophysical Research Letters, 43, 5741–5749, https://doi.org/10.1002/2016GL068972, 2016.

Chuter, S. J., Martín-Español, A., Wouters, B., and Bamber, J. L.: Mass balance reassessment of glaciers draining into the Abbot and Getz Ice Shelves of West Antarctica, Geophysical Research Letters, 44, 7328–7337, https://doi.org/10.1002/2017GL073087, 2017.

ESA AIS CCI: Grounding line for key glaciers, Antarctica, derived from ERS-1/2, TerraSAR-X and Copernicus Sentinel-1 data acquired in 1994-2021, https://climate.esa.int/en/projects/ice-sheets-antarctic/, 2021.

Freer, B. I. D., Marsh, O. J., Hogg, A. E., Fricker, H. A., and Padman, L.: Modes of Antarctic tidal grounding line migration revealed by Ice, Cloud, and land Elevation Satellite-2 (ICESat-2) laser altimetry, The Cryosphere, 17, 4079–4101, https://doi.org/10.5194/tc-17-4079-2023, 2023.

Fricker, H. A. and Padman, L.: Ice shelf grounding zone structure from ICESat laser altimetry, Geophysical Research Letters, 33, 2006GL026 907, https://doi.org/10.1029/2006GL026907, 2006.

Friedl, P., Weiser, F., Fluhrer, A., and Braun, M. H.: Remote sensing of glacier and ice sheet grounding lines: A review, Earth-Science Reviews, 201, 102 948, https://doi.org/10.1016/j.earscirev.2019.102948, 2020.

Gourmelen, N., Jakob, L., Holland, P. R., Dutrieux, P., Goldberg, D., Bevan, S., Luckman, A., and Malczyk, G.: The influence of subglacial lake discharge on Thwaites Glacier ice-shelf melting and grounding-line retreat, Nature Communications, 16, 2272, https://doi.org/10.1038/s41467-025-57417-1, 2025.

Holland, P. R., Bevan, S. L., and Luckman, A. J.: Strong Ocean Melting Feedback During the Recent Retreat of Thwaites Glacier, Geophysical Research Letters, 50, e2023GL103 088, https://doi.org/10.1029/2023GL103088, 2023.

Howat, I., Porter, C., Noh, M.-J., Husby, E., Khuvis, S., Danish, E., Tomko, K., Gardiner, J., Negrete, A., Yadav, B., Klassen, J., Kelleher, C., Cloutier, M., Bakker, J., Enos, J., Arnold, G., Bauer, G., Morin, P., and Polar Geospatial Center: The Reference Elevation Model of Antarctica - Mosaics, Version 2, https://doi.org/10.7910/DVN/EBW8UC, 2022.

Joughin, I., Smith, B. E., and Holland, D. M.: Sensitivity of 21st century sea level to ocean-induced thinning of Pine Island Glacier, Antarctica, Geophysical Research Letters, 37, 2010GL044 819, https://doi.org/10.1029/2010GL044819, 2010.

Joughin, I., Smith, B. E., and Medley, B.: Marine Ice Sheet Collapse Potentially Under Way for the Thwaites Glacier Basin, West Antarctica, Science, 344, 735–738, https://doi.org/10.1126/science.1249055, 2014.

Konrad, H., Shepherd, A., Gilbert, L., Hogg, A. E., McMillan, M., Muir, A., and Slater, T.: Net retreat of Antarctic glacier grounding lines, Nature Geoscience, 11, 258–262, https://doi.org/10.1038/s41561-018-0082-z, 2018.

Le Meur, E., Sacchettini, M., Garambois, S., Berthier, E., Drouet, A. S., Durand, G., Young, D., Greenbaum, J. S., Holt, J. W., Blankenship, D. D., Rignot, E., Mouginot, J., Gim, Y., Kirchner, D., De Fleurian, B., Gagliardini, O., and Gillet-Chaulet, F.: Two independent methods for mapping the grounding line of an outlet glacier – an example from the Astrolabe Glacier, Terre Adélie, Antarctica, The Cryosphere, 8, 1331–1346, https://doi.org/10.5194/tc-8-1331-2014, 2014.

Li, T., Dawson, G. J., Chuter, S. J., and Bamber, J. L.: Grounding line retreat and tide-modulated ocean channels at Moscow University and Totten Glacier ice shelves, East Antarctica, The Cryosphere, 17, 1003–1022, https://doi.org/10.5194/tc-17-1003-2023, 2023.

Massonnet, D., Rossi, M., Carmona, C., Adragna, F., Peltzer, G., Feigl, K., and Rabaute, T.: The displacement field of the Landers earthquake mapped by radar interferometry, Nature, 364, 138–142, https://doi.org/10.1038/364138a0, 1993.

Milillo, P., Rignot, E., Rizzoli, P., Scheuchl, B., Mouginot, J., Bueso-Bello, J., and Prats-Iraola, P.: Heterogeneous retreat and ice melt of Thwaites Glacier, West Antarctica, Science Advances, 5, eaau3433, https://doi.org/10.1126/sciadv.aau3433, 2019.

Milillo, P., Rignot, E., Rizzoli, P., Scheuchl, B., Mouginot, J., Bueso-Bello, J. L., Prats-Iraola, P., and Dini, L.: Rapid glacier retreat rates observed in West Antarctica, Nature Geoscience, 15, 48–53, https://doi.org/10.1038/s41561-021-00877-z, 2022.

Millan, R., Mouginot, J., Derkacheva, A., Rignot, E., Milillo, P., Ciraci, E., Dini, L., and Bjørk, A.: Ongoing grounding line retreat and fracturing initiated at the Petermann Glacier ice shelf, Greenland, after 2016, The Cryosphere, 16, 3021–3031, https://doi.org/10.5194/tc-16-3021-2022, 2022.

Mohajerani, Y., Jeong, S., Scheuchl, B., Velicogna, I., Rignot, E., and Milillo, P.: Automatic delineation of glacier grounding lines in differential interferometric synthetic-aperture radar data using deep learning, Scientific Reports, 11, 4992, https://doi.org/10.1038/s41598-021-84309-3, 2021.

Morlighem, M.: MEaSUREs BedMachine Antarctica, Version 3, https://doi.org/10.5067/FPSU0V1MWUB6, 2022.

Morlighem, M., Rignot, E., Binder, T., Blankenship, D., Drews, R., Eagles, G., Eisen, O., Ferraccioli, F., Forsberg, R., Fretwell, P., Goel, V., Greenbaum, J. S., Gudmundsson, H., Guo, J., Helm, V., Hofstede, C., Howat, I., Humbert, A., Jokat, W., Karlsson, N. B., Lee, W. S., Matsuoka, K., Millan, R., Mouginot, J., Paden, J., Pattyn, F., Roberts, J., Rosier, S., Ruppel, A., Seroussi, H., Smith, E. C., Steinhage, D., Sun, B., Broeke, M. R. V. D., Ommen, T. D. V., Wessem, M. V., and Young, D. A.: Deep glacial troughs and stabilizing ridges unveiled beneath the margins of the Antarctic ice sheet, Nature Geoscience, 13, 132–137, https://doi.org/10.1038/s41561-019-0510-8, 2020.

Mouginot, J., Rignot, E., and Scheuchl, B.: Sustained increase in ice discharge from the Amundsen Sea Embayment, West Antarctica, from 1973 to 2013, Geophysical Research Letters, 41, 1576–1584, https://doi.org/10.1002/2013GL059069, 2014.

Otosaka, I. N., Shepherd, A., Ivins, E. R., Schlegel, N.-J., Amory, C., Van Den Broeke, M. R., Horwath, M., Joughin, I., King, M. D., Krinner, G., Nowicki, S., Payne, A. J., Rignot, E., Scambos, T., Simon, K. M., Smith, B. E., Sørensen, L. S., Velicogna, I., Whitehouse, P. L., A, G., Agosta, C., Ahlstrøm, A. P., Blazquez, A., Colgan, W., Engdahl, M. E., Fettweis, X., Forsberg, R., Gallée, H., Gardner, A., Gilbert, L., Gourmelen, N., Groh, A., Gunter, B. C., Harig, C., Helm, V., Khan, S. A., Kittel, C., Konrad, H., Langen, P. L., Lecavalier, B. S., Liang, C.-C., Loomis, B. D., McMillan, M., Melini, D., Mernild, S. H., Mottram, R., Mouginot, J., Nilsson, J., Noël, B., Pattle, M. E., Peltier, W. R., Pie, N., Roca, M., Sasgen, I., Save, H. V., Seo, K.-W., Scheuchl, B., Schrama, E. J. O., Schröder, L., Simonsen, S. B., Slater, T., Spada, G., Sutterley, T. C., Vishwakarma, B. D., Van Wessem, J. M., Wiese, D., Van Der Wal, W., and Wouters, B.: Mass balance of the Greenland and Antarctic ice sheets from 1992 to 2020, Earth System Science Data, 15, 1597–1616, https://doi.org/10.5194/essd-15-1597-2023, 2023.

Park, J. W., Gourmelen, N., Shepherd, A., Kim, S. W., Vaughan, D. G., and Wingham, D. J.: Sustained retreat of the Pine Island Glacier, Geophysical Research Letters, 40, 2137–2142, https://doi.org/10.1002/grl.50379, 2013.

Qian, Y., Zhou, C., Sun, S., Chen, Y., Wang, T., and Zhang, B.: Ephemeral grounding on the Pine Island Ice Shelf, West Antarctica, from 2014 to 2023, https://doi.org/10.5194/egusphere-2025-603, 2025.

Rignot, E.: Tidal motion, ice velocity and melt rate of Petermann Gletscher, Greenland, measured from radar interferometry, Journal of Glaciology, 42, 476–485, https://doi.org/10.3189/S0022143000003464, 1996.

Rignot, E.: Observations of grounding zones are the missing key to understand ice melt in Antarctica, Nature Climate Change, 13, 1010–1013, https://doi.org/10.1038/s41558-023-01819-w, 2023.

Rignot, E., Mouginot, J., Morlighem, M., Seroussi, H., and Scheuchl, B.: Widespread, rapid grounding line retreat of Pine Island, Thwaites, Smith, and Kohler glaciers, West Antarctica, from 1992 to 2011, Geophysical Research Letters, 41, 3502–3509, https://doi.org/10.1002/2014GL060140, 2014.

Rignot, E., Mouginot, J., and Scheuchl, B.: MEaSUREs Antarctic Grounding Line from Differential Satellite Radar Interferometry, Version 2, https://doi.org/10.5067/IKBWW4RYHF1Q, 2016.

Rignot, E., Mouginot, J., and Scheuchl, B.: MEaSUREs InSAR-Based Antarctica Ice Velocity Map, Version 2, https://doi.org/10.5067/D7GK8F5J8M8R, 2017.

Rignot, E., Ciracì, E., Scheuchl, B., Tolpekin, V., Wollersheim, M., and Dow, C.: Widespread seawater intrusions beneath the grounded ice of Thwaites Glacier, West Antarctica, Proceedings of the National Academy of Sciences, 121, e2404766 121, https://doi.org/10.1073/pnas.2404766121, 2024.

Scheuchl, B., Mouginot, J., Rignot, E., Morlighem, M., and Khazendar, A.: Grounding line retreat of Pope, Smith, and Kohler Glaciers, West Antarctica, measured with Sentinel-1a radar interferometry data, Geophysical Research Letters, 43, 8572–8579, https://doi.org/10.1002/2016GL069287, 2016.

Schmidtko, S., Heywood, K. J., Thompson, A. F., and Aoki, S.: Multidecadal warming of Antarctic waters, Science, 346, 1227–1231, https://doi.org/10.1126/science.1256117, 2014.

Selley, H. L., Hogg, A. E., Davison, B. J., Dutrieux, P., and Slater, T.: Speed-up, slowdown, and redirection of ice flow on neighbouring ice streams in the Pope, Smith, and Kohler region of West Antarctica, The Cryosphere, 19, 1725–1738, https://doi.org/10.5194/tc-19-1725-2025, 2025.